# Upregulation of Caveolae-Associated Proteins in Lesional Samples of Hidradenitis Suppurativa: A Case Series Study

Neil Seth[1], Beatriz Abdo Abujamra[1], Maria Boulina[2], Hadar Lev-Tov[1] and Ivan Jozic[1]

Hidradenitis suppurativa (HS) is a chronic, inflammatory skin condition. HS disease management has proven difficult owing to an insufficient understanding of the immunological processes that drive its pathogenesis. We have demonstrated that misregulation of caveolae perturbs inflammatory responses, inhibits cutaneous wound healing, and contributes to immune privilege collapse in other hair follicle−related diseases. However, nothing is known about its role or the role of structural components of caveolae (caveolin [Cav1] 1, Cav2, and Cavin-1) in the pathophysiology of HS. We aimed to identify whether Cav1, Cav2, and Cavin-1 may serve as immuno-histochemical markers of HS. Lesional and perilesional HS skin samples from patients (n = 7, mean age = 35.7 years, range = 20−57 years) with active HS and normal skin from control participants (n = 4, mean age = 36.7 years, range = 23−49 years) were used to assess Cav1, Cav2, and Cavin-1 expression and localization by immunofluorescence staining. HS samples demonstrated increased levels of Cav1 compared with normal skin, whereas Cav1, Cav2, and Cavin-1 were all elevated in hair follicles of lesional versus perilesional HS samples, suggesting a potentially novel therapeutic target and highlighting caveolae as potential biomarkers of HS.

## INTRODUCTION

Hidradenitis suppurativa (HS) is a chronic, inflammatory skin condition characterized by painful nodules, abscesses, sinus tracts, and scar formation in intertriginous and apocrine gland-rich areas of the body (Napolitano et al., 2017). Patients with HS exhibit a significantly diminished QOL, with the disease disproportionally affecting young adults, women, and African Americans (Schneider-Burrus et al., 2021). In Western countries, HS affects 1% of the population, with annual incidence rates rising over the last decade (Garg et al., 2017; Ingram, 2020). Although therapeutic management of HS is difficult mostly owing to the limited understanding of its pathogenesis (Amat-Samaranch et al., 2021), the pilosebaceous−apocrine unit has remained the recognized skin component that hosts HS (Narla et al., 2020), with initial work highlighting apocrine glands as the initial target in HS development (Yu and Cook, 1990) and more recent work centering around the hair follicle (HF) (Chen and Plewig, 2017; Zouboulis et al., 2020). Histologically, the events initiating HS include perifollicular immune cell infiltration, excess keratin production, and epidermal hyperplasia of the follicular infundibulum (von Laffert et al., 2010; Wolk et al., 2020; Yu and Cook, 1990), resulting in follicular occlusion with subsequent dilation and stasis of the HF (Castelli et al., 2022; Sabat et al., 2020; Wolk et al., 2020). Notably, real-time confocal microscopy efforts have further characterized the morphological changes of the follicular unit in HS lesional samples, noting increased size of infundibular diameter, amount of material within infundibula, and keratinization of the follicular border (Cappilli et al., 2021). Furthermore, diminished quiescent stem cells and increased proliferating progenitor cells have been identified upon examination of HF stem cells collected from HS lesions (Orvain et al., 2020).

The immunological processes that mediate HS development are varied, numerous, and complex. Several mediators of microbial-induced inflammation have been identified, including antimicrobial peptides such as cathelicidin (LL-37) and human β-defensin (Emelianov et al., 2012). Multiple proinflammatory cytokines contribute to the immune dysregulation in HS, with numerous studies showing increased levels of TNF-α, IL-1ß, IL-17, and IFN-γ in HS lesions (Kelly et al., 2015; van der Zee et al., 2011). Inflammation is further exacerbated by dysregulation of macrophages, in response to proinflammatory cytokines. Finally, the immunological profile of HS also includes the involvement of T helper cells, with dysregulation of T helper 17 cells, regulatory T cells, and T helper 1 cells (Moran et al., 2017; Napolitano et al., 2017). Previous studies have also demonstrated increased levels of complement C5a in serum and tissue that correlate with disease activity and degree of neutrophilic infiltrates, suggesting a role for the complement system in HS pathophysiology as well (Riedemann et al., 2017).

[1]Dr. Phillip Frost Department of Dermatology and Cutaneous Surgery, University of Miami Miller School of Medicine, Miami, Florida, USA; and [2]Diabetes Research Institute, University of Miami Miller School of Medicine, Miami, Florida, USA

Correspondence: Ivan Jozic, Dr. Phillip Frost Department of Dermatology and Cutaneous Surgery, University of Miami Miller School of Medicine, 1600 Northwest 10th Avenue, RMSB 2089, Miami, Florida 33136, USA. E-mail: i.jozic@med.miami.edu

Although numerous advancements in pharmacotherapy have improved the options available to patients with HS, there is still no uniformly effective treatment, and management remains complex. Moreover, properly identifying HS has remained a great challenge to providers, with many cases resulting in misdiagnosis or a significant time delay to proper diagnosis. On average, patients with HS have a delay of 7 years between symptom onset and establishment of a diagnosis (Jemec and Kimball, 2015). Currently, there is no reliable biomarker for the disease, and severity staging relies on imperfect clinical scoring scales. Fortunately, studies geared toward closing knowledge gaps, improving diagnostic and prognostic methods, and developing efficacious therapies continue to gain momentum and advance how clinicians treat HS.

Interestingly, caveolae (a unique class of flask-shaped, cell membrane–based lipid rafts that are rich in cholesterol and sphingomyelin) have emerged as mechanical sensors and mediators of various cellular signal transduction events, with roles in diseases ranging from atherosclerosis to cancer (Parton and del Pozo, 2013). Caveolae play an important role in helping the cell membrane pinch off a segment of the membrane and form carrier vessels that result in internalization of cargo through endomembrane trafficking. Caveolin (Cav) proteins are the primary structural components of caveolae and allow for alterations in cellular signaling and modulation of numerous downstream targets (Cohen et al., 2004). Cav1 has been demonstrated to be at least tangentially involved in skin physiology, being linked to cell proliferation and migration, infection, and inflammation, and as such, there is some evidence (utilizing murine and human tissues) associating it with various cutaneous diseases, including psoriasis, fibrosis, cicatricial alopecia, basal and squamous cell carcinoma, melanoma, and chronic wound healing (reviewed in Egger et al. [2020]). To this end, we have previously demonstrated that acute wounds exhibit a spatiotemporal downregulation of Cav1 at their wound edge, whereas at least two types of nonhealing chronic wounds (diabetic foot and venous leg ulcers) exhibit upregulation of Cav1 expression at their wound edge, which serves to sequester GF receptors and thus antagonizes downstream signaling through these receptors (Castellanos et al., 2020; Jozic et al., 2021a, 2019; Sawaya et al., 2019). Notably, past work has demonstrated that Cav1 can regulate NF-κB activation through effects on downstream enzymes such as endothelial nitric oxide synthase, resulting in a blunted inflammatory response to lipopolysaccharide (Garrean et al., 2006). Importantly, Cav1 has also been previously shown to colocalize with toll-like receptor 4 and augment inflammatory response in murine macrophages (Wang et al., 2009). However, the role of Cav1 in inflammatory response seems to be cell context dependent. Recent reports demonstrate that Cav1-deficient cells under metabolic stress conditions exhibit improved NF-κB signaling mediated through GPRC5B, which displays great binding affinity to Cav1 and has implications in obesity-linked inflammation (Kim and Hirabayashi, 2018). Other caveolae-associated proteins (including Cav2 and Cavin-1 [PTRF]) have demonstrated a multitude of roles in human disease processes and may also participate in inflammatory signaling; however, their role in cutaneous physiology is largely unknown (Chidlow and Sessa, 2010; Cohen et al., 2004).

Therefore, we hypothesized that caveolar abundance and expression of its structural components (Cav1, Cav2, and Cavin-1) may be altered in the skin of people with HS. In this paper, we report a case series, in which we investigate and quantify the expression and localization of caveolae-associated structural proteins Cav1, Cav2, and Cavin-1 in lesional and perilesional skin samples of seven patients with HS. We aim at understanding the role of caveolae-associated structural proteins in the pathophysiology of HS and highlight a potential avenue for developing improved prognostic approaches and treatment strategies by targeting these specialized membrane microdomains.

## CASE SERIES REPORT

Discarded skin from seven subjects with advanced Hurley-stage HS (average age = $35.7 \pm 15.1$ years) was obtained from excisions performed on either the right or left axilla, abdomen, or groin. Normal abdominal skin samples were obtained from four participants, and a comparison of lesional and perilesional HS skin sample locations was conducted in three of the seven participants. The majority of the subjects with HS were female (6 of 7), with 50% identifying as smokers (and one unreported), five of seven identifying as Hurley stage 3, and two of seven identifying as Hurley stage 2 (Table 1). Expression of Cav1, Cav2, and Cavin1 was performed through immunofluorescence microscopy, and relative localization was qualified by localization to keratin (K) 10- and K15-positive regions of the tissue. Skin samples from patients with lesions with HS (n = 4) demonstrated increased expression of Cav1 compared with age-matched control abdominal skin samples (n = 4) (Figure 1a). Moreover, they exhibited mislocalization of Cav1 beyond the basal keratinocytes as evidenced by localizing to K10$^+$ areas of the epidermis (Figure 1b). Interestingly, three of four lesional HS samples exhibited elevated inflammatory cell infiltrate that stained positive for Cav1 (Figure 1c).

To characterize the potential differences in the expression of caveolae-associated proteins in lesional versus perilesional skin of patients with HS (n = 3), lesional and perilesional specimens from the same patient were costained against either Cav1, Cav2, or Cavin-1 with K10. We found a statistically significant increase in Cav1 expression between both normal skin and perilesional HS as well as between perilesional and lesional HS (n =3; one-way ANOVA, $P < 0.001$) (Figure 2). Although perilesional HS skin samples exhibited increased levels of Cav1, they did not demonstrate altered localization of Cav1 beyond K10-positive areas as exhibited by lesional HS skin samples (Figure 2a and b). Because we have previously demonstrated that Cav1 localizes to the outer root sheath cells of the HF bulge (which are K15$^+$) (Jozic et al., 2021b) and because other studies have proposed HS as an HF-related disease, we wanted to extend our findings beyond the epidermis and thus sought to delineate expression and localization of Cav1, Cav2, and Cavin-1 in the HF. First, we observed that in the lesional HS samples, Cav1 localizes not only to K15$^+$ regions within the HF but also beyond the outer root sheath (Figure 2b). Moreover, Cav2 and Cavin1 both exhibited elevated levels in perilesional and lesional HS

## Table 1. Demographics of Human Skin Samples

| Subject | Sex | Age | Location | Hurley Stage | Smoker |
|---|---|---|---|---|---|
| Normal skin samples | | | | | |
| #001 | F | 23 | Abdomen | — | — |
| #002 | F | 27 | Abdomen | — | — |
| #003 | F | 48 | Abdomen | — | — |
| #004 | F | 49 | Abdomen | — | — |
| #005 | F | 53 | Scalp | — | — |
| #006 | F | 51 | Scalp | — | — |
| #007 | F | 54 | Scalp | — | — |
| HS samples | | | | | |
| #001 | F | 20 | Right axilla | 2 | Y |
| #002 | M | 26 | Left axilla | 3 | n/a |
| #003 | F | 48 | Left flank | 3 | Y |
| #004 | F | 49 | Left axilla | 3 | Y |
| #005 | F | 23 | Abdomen (lesional vs. perilesional) | 3 | N |
| #006 | F | 57 | Groin (lesional vs. perilesional) | 2 | Y |
| #007 | F | 27 | Axilla (lesional vs. perilesional) | 3 | N |

Abbreviations: #, number; F, female; HS, hidradenitis suppurativa; M, male; N, no; n/a, not available; Y, yes.
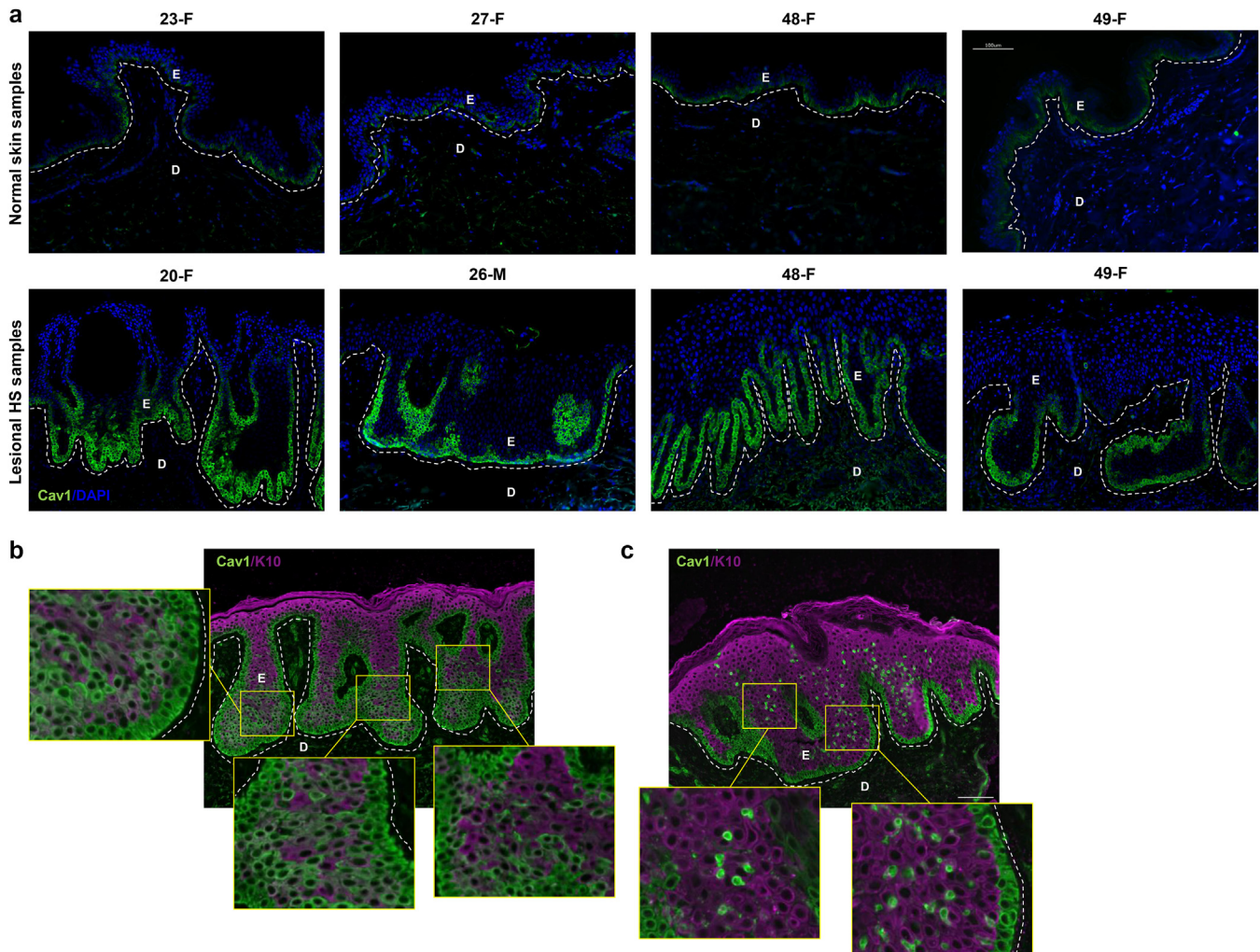


Figure 1. Elevated expression and mislocalization of Cav1 in the skin of patients with HS. (a) Skin samples from n = 4 patients with HS were immunostained against Cav1 (green), counterstained with DAPI (blue), and expression was compared with that of normal abdominal skin samples (n = 4) (E denotes the epidermis; D denotes the dermis). (b, c) Representative images of HS skin samples coimmunostained against Cav1 (green) and K10 (magenta), confirming mislocalization of Cav1 to suprabasal (K10-positive) layers of the epidermis. Bar = 100 μm. Cav1, caveolin-1; F, female; HS, hidradenitis suppurativa; K10, keratin 10; M, male.
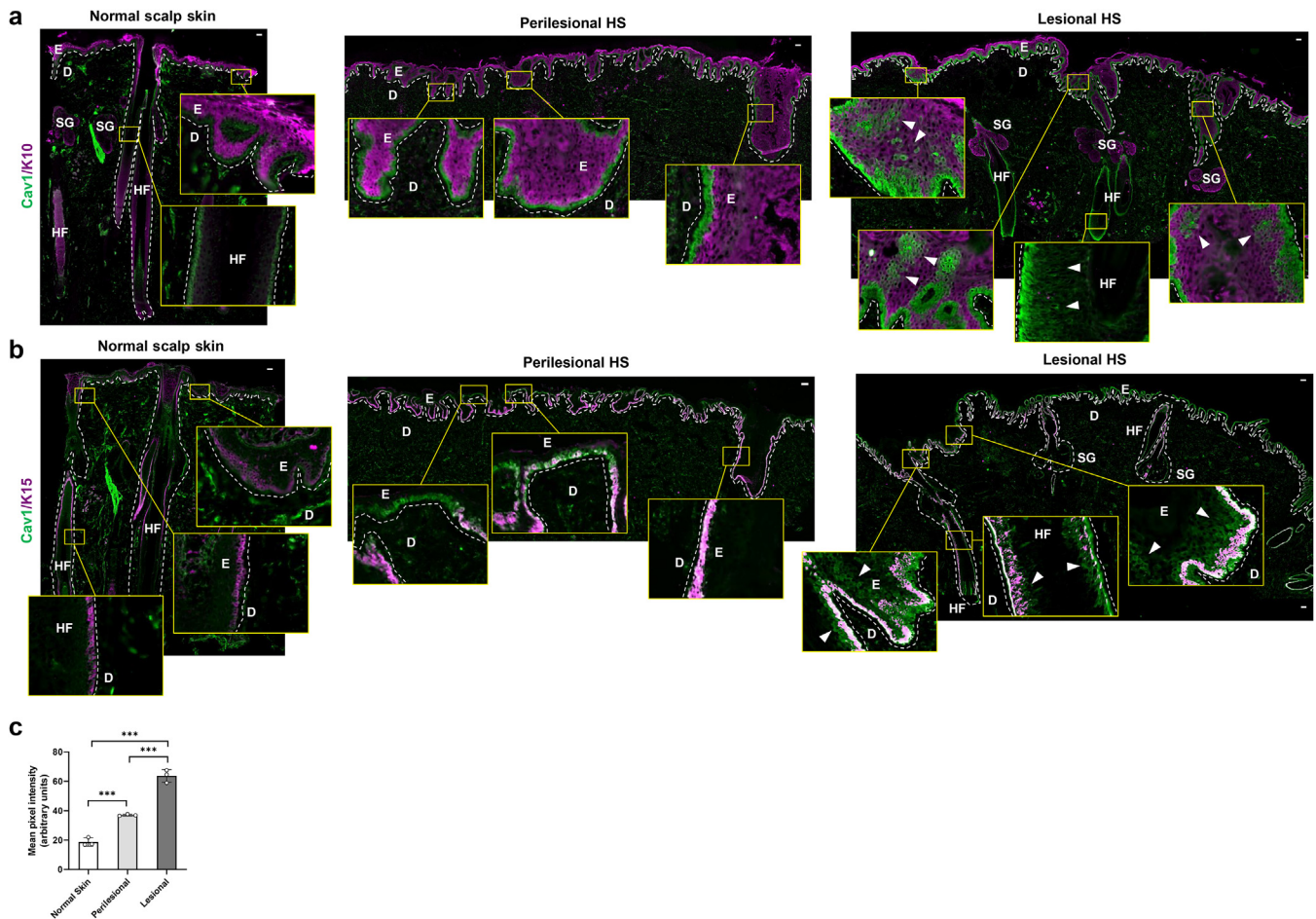
**Figure 2. Elevated expression of Cav1 in lesional skin of patients with HS.** Representative images of normal control scalp skin (n = 3) comparing expression with that of either lesional or perilesional skin samples from the same patient with HS (n = 3) that were immunostained against Cav1 (green) and counterstained with either (**a**) K10 or (**b**) K15 (magenta) (white arrowheads point to areas of mislocalization of Cav1). (**c**) Quantification of Cav1 staining using mean pixel intensity over area. Error bars correspond to SD from n = 3 biological replicates. ***$P < 0.001$. One-way ANOVA with Tukey's posthoc test was used for multiple pairwise comparisons (bar = 100 μm). Cav1, caveolin-1; D, dermis; E, epidermis; HF, hair follicle; HS, hidradenitis suppurativa; K, keratin; SG, stratum granulosum.

samples (resembling what we saw with Cav1) as well as changes in localization with respect to K10- and K15-positive areas (Figures 3 and 4), suggesting a conserved effect for all caveolae-associated proteins. To confirm that this is specific to caveolae-associated proteins and not components of other endocytic machinery, we isolated proteins from normal skin as well as from perilesional and lesional HS samples and performed immunoblotting against Cav1 and clathrin. Indeed, we found that the observed increase in Cav1 expression did not extend to clathrin (Figure 5).

## DISCUSSION

In this case series report, we identified the upregulation of caveolae-associated proteins in lesional samples of patients with HS, a disease pathophysiologically characterized by chronic inflammatory disruption. Intriguingly, we demonstrated that perilesional skin from patients with HS exhibited increased expression of caveolae-associated proteins (Cav1, Cav2, and Cavin1) compared with normal skin, whereas lesional HS skin samples exhibited significantly elevated levels of the same structural components, in comparison with perilesional skin from the same patient. The gradual increase

in caveolar proteins in perilesional and striking increase in lesional HS skin samples (in comparison with that in normal skin) suggests that deregulation of these structural components may act as a nodus that allows for perturbation of local microenvironment and may lead to dysbiosis of the normal skin flora because Cavs have been previously demonstrated to associate with internalization of various bacteria. We are actively exploring how Cav1 binds to and alters the availability and downstream signaling of numerous toll-like receptors and hope to report on these findings in the near future. Interestingly, the apparent mislocalization of Cav1 in the HF may also lead to disruption of quiescence in the stem cell bulge of the HF and may lead to aberrant proliferation of keratinocytes within this HF niche.

Although the sample size is limited, our findings support a growing trend that distinguishes Cav1 as an immunomodulatory role player, which disturbs the inflammatory balance of effective wound healing. Likewise, although we did our best to age/sex match our control skin samples to HS samples, our normal skin samples were restricted to the abdominal and scalp skin, whereas HS samples included the axilla, flank abdomen, and groin. We understand the limit
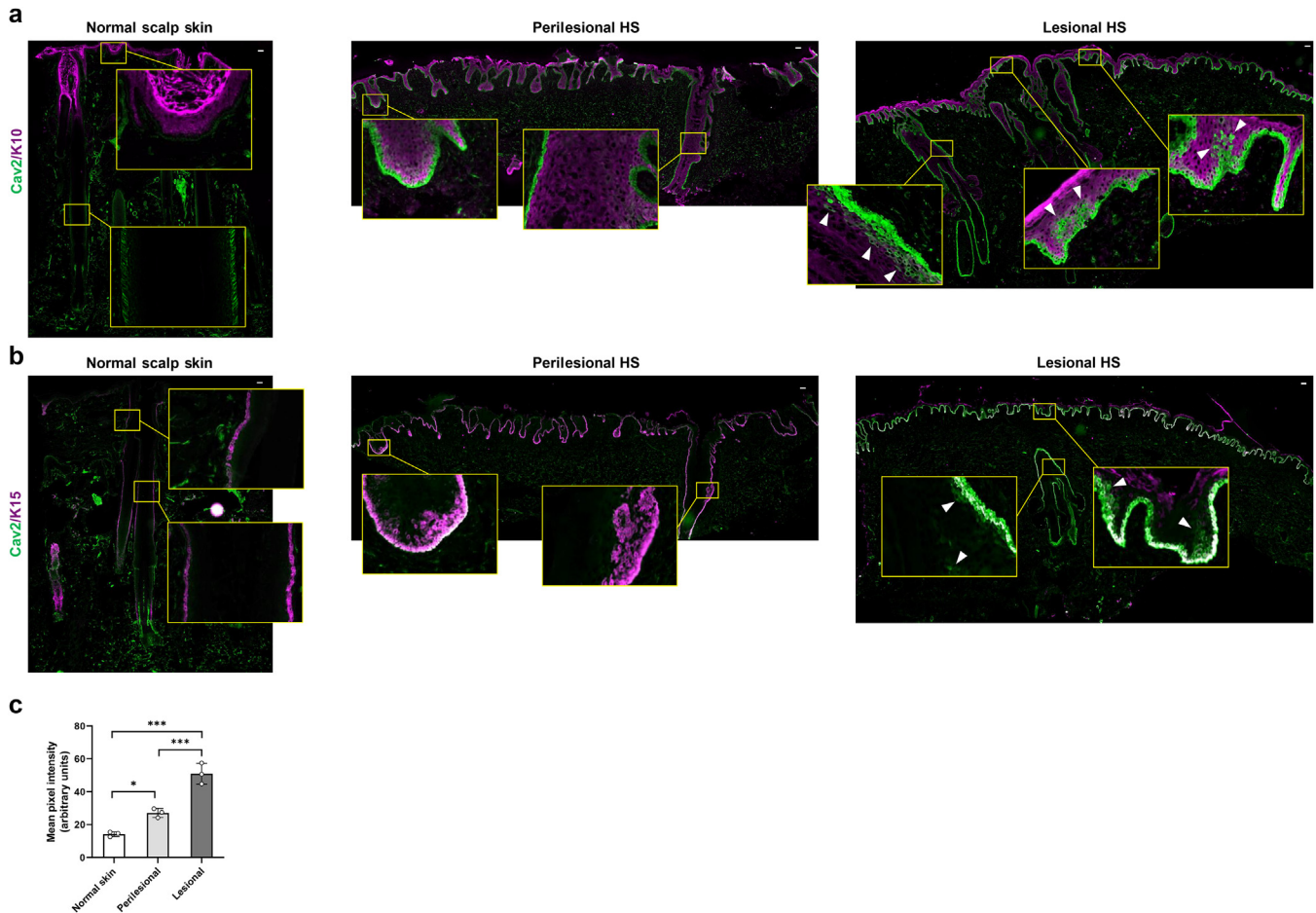
**Figure 3. Elevated expression of Cav2 in lesional skin of patients with HS.** Representative images of normal control skin comparing expression with that of either lesional or perilesional skin samples from the same patient with HS (n = 3) that were immunostained against Cav2 (green) and counterstained with either (**a**) K10 or (**b**) K15 (magenta) (white arrowheads point to areas of mislocalization of Cav1). (**c**) Quantification of Cav1 staining using mean pixel intensity over area. Error bars correspond to SD from n = 3 biological replicates. *$P < 0.05$ and ***$P < 0.001$. One-way ANOVA with Tukey's posthoc test was used for multiple pairwise comparisons (bar = 100 μm). Cav2, caveolin-2; HS, hidradenitis suppurativa; K, keratin.

this imposes on our interpretation of observed results, and we hope to include more precise location-matched samples going forward.

The differential expression of Cav1 in lesional versus perilesional HS tissue interestingly parallels the trend of Cav1 expression demonstrated in nonhealing diabetic foot and venous leg ulcers, which we have previously demonstrated to exhibit upregulation of Cav1 at their wound edge (Jozic et al., 2021a, 2019; Sawaya et al., 2019). Moreover, others have shown that deregulation of Cav1 may also perturb both the response to and output from cellular events that classically excite an inflammatory response (Garrean et al., 2006; Kim and Hirabayashi, 2018; Tsai et al., 2018; Wang et al., 2009). In addition, we have previously demonstrated that Cav1 is upregulated and mislocalized in other HF-related diseases, including frontal fibrosing alopecia, where we posit that it facilitates immune privilege collapse of the epithelial HF stem cells (Jozic et al., 2021b). Owing to the correlative nature of the demonstrated results in lesional HS samples, it is impossible to conclude whether Cav1 is the driver of HS pathophysiology or a consequence of the disease. Regardless, Cav1 still may hold an important clinical role as a potential biomarker of HS progression; however, a

much larger sample size will be necessary to substantiate this hypothesis. Therefore, further investigation geared toward uncovering the role of caveolae-associated proteins may continue to elucidate the inflammatory disarray that underlies HS pathophysiology. Fascinatingly, increased upregulation of Cav1 at the wound edge identified in previous work, alongside our findings of differentially increased upregulation of Cav1 in lesional versus perilesional tissue, brings forth Cav1 as an attractive area of focus for the development of novel theragnostic targets for treatment of HS.

## METHODS
### Study design
This case series investigated and quantified the expression of caveolae-associated proteins Cav1, Cav2, and Cavin-1 in lesional and perilesional skin samples of seven patients with active HS. The research protocols for the case series were reviewed and approved by the University of Miami Institutional Review Board (Institutional Review Board number 20200187); however, because only deidentified discarded tissue was collected, no consent is required because this is not considered human subject research. Normal skin specimens were obtained as discarded tissue from voluntary surgical
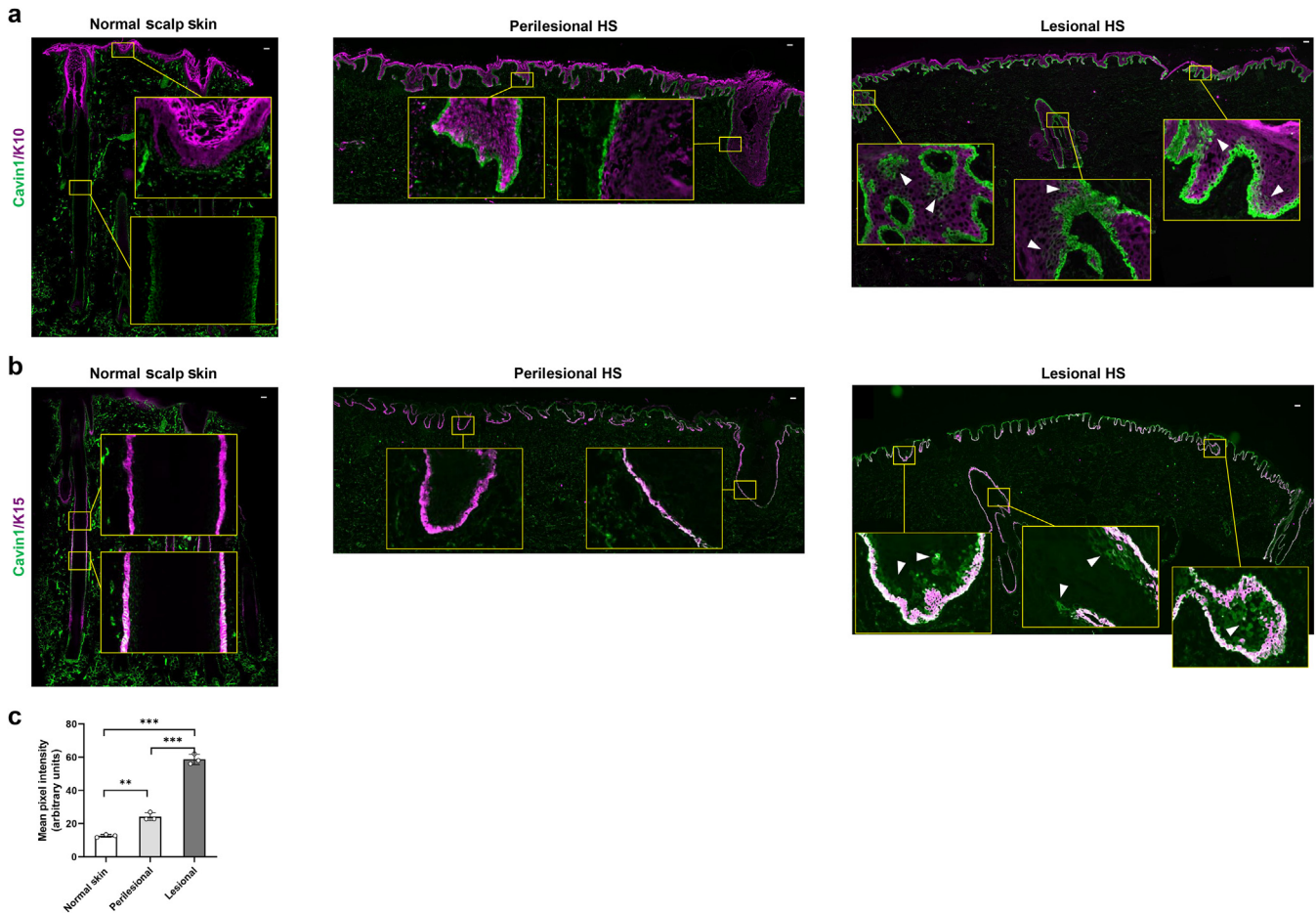
**Figure 4. Elevated expression of Cavin-1 in lesional skin of patients with HS.** Representative images of normal control skin comparing expression with that of either lesional or perilesional skin samples from the same patient with HS (n = 3) that were immunostained against either Cavin-1 (green) and counterstained with either (**a**) K10 or (**b**) K15 (magenta) (white arrowheads point to areas of mislocalization of Cav1). (**c**) Quantification of Cav1 staining using mean pixel intensity over area. Error bars correspond to SD from n = 3 biological replicates. **$P < 0.01$ and ***$P < 0.001$. One-way ANOVA with Tukey's posthoc test was used for multiple pairwise comparisons (bar = 100 μm; Cavin1 is also known as PTRF). Cav1, caveolin-1; HS, hidradenitis suppurativa; K, keratin.

excision of nondiseased abdominal skin. HS subjects were recruited from an outpatient HS specialty clinic at the University of Miami (Miami, Florida) with active HS of at least 1-year duration with minimum disease severity of Hurley stage II, where discarded tissue from lesional and perilesional skin specimens after local excisional procedures were performed as part of standard care. Lesional skin

was defined as the edge of an inflammatory lesion, and perilesional skin was defined as normal-appearing skin 2 cm away from the inflammatory lesion (Frew et al., 2019). Upon retrieval in the medical clinic, skin samples were immediately frozen in liquid nitrogen for storage and transport.
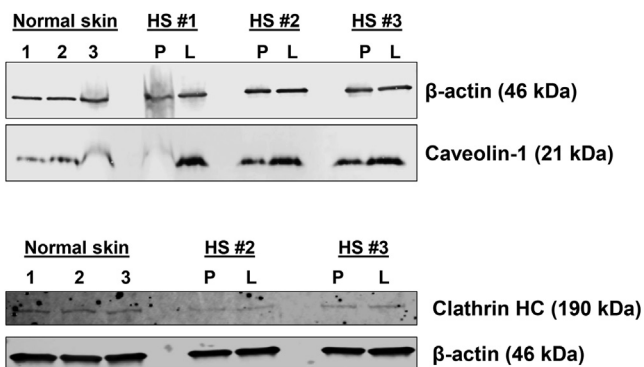
## Immunofluorescence staining and quantification

Tissue samples were cryosectioned at 5 μm and fixed with 10% formaldehyde for 10 minutes at room temperature, followed by three washes with tris-buffered saline. Slides containing sections were then incubated with Image-iT FX Signal Enhancer (number I36933, Molecular Probes, Eugene, OR) for 30 minutes and incubated overnight at 4 °C with primary antibodies diluted in 5% normal goat serum supplemented with 0.05% tween-20 (Cav1: 1:200 [Sigma-Aldrich, St. Louis, MO, number HPA049326]; Cav2: 1:200 [Sigma-Aldrich, number HPA044810]; Cavin1: 1:500 [Cell Signaling Technology, Danvers, MA, number 69036]; K10: 1:400 [Santa Cruz Biotechnology, Dallas, TX, sc23877]; and K15: 1:300 [Santa Cruz Biotechnology, sc47697]). Samples were washed three times with tris-buffered saline supplemented with 0.05% tween-20 and once with tris-buffered saline before incubating with Alexa Flour 488—conjugated anti-rabbit antibody or Alexa Fluor 594—conjugated anti-mouse secondary antibodies (1:300) and mounted with ProLong



**Figure 5. HS skin samples do not exhibit changes in levels of clathrin.** Relative levels of Cav1 and clathrin HC were assessed by immunoblotting, with β-actin serving as loading control. P denotes perilesional HS samples, and L denotes lesional HS samples. Cav1, caveolin-1; HC, heavy chain; HS, hidradenitis suppurativa.

Gold Antifade mounting media with DAPI (Thermo Fisher Scientific, Waltham, MA). Images were captured and analyzed using Keyence BZ-X700 inverted microscope and Olympus VS120 slide scanner. Expression of Cav1, Cav2, and Cavin-1 in the skin of patients with HS was visualized and demonstrated across the captured immunofluorescence images. To make the figures accessible to readers with color blindness, red channel was replaced with magenta.

### Immunoblotting

To isolate protein, skin samples were washed twice with ice-cold PBS and lysed in ice-cold lysis buffer (20 mM Tris-hydrogen chloride, pH 7.5, 150 mM sodium chloride, 1% Triton X-100) (Jozic et al., 2021a). The lysates were clarified by centrifugation, and protein concentrations were determined using the BCA Protein Assay Reagent Kit (Thermo Fisher Scientific). Proteins were resolved by 4−20% Criterion TGX pre-cast gels (Bio-Rad Laboratories, Hercules, CA), transferred to polyvinylidene difluoride membranes (Thermo Fisher Scientific), and placed in blocking buffer for 1 hour (tris-buffered saline, 0.1% Tween-20, 5% BSA) and then probed with rabbit anti-Cav1 (number 3267, 1:2,000, Cell Signaling Signaling), rabbit anti-clathrin HC (number 4796, 1:500, Cell Signaling Signaling), and mouse anti−β-actin (number A5441, 1:20,000, Sigma-Aldrich) antibodies overnight, followed by exposure to near either goat anti-mouse IR680 (LI-COR Biosciences, Lincoln, NE, number 926-68070, 1:15,000, reactive toward mouse $IgG_1$, $IgG_{2a}$, $IgG_{2b}$, and $IgG_3$ heavy/light chains and light chains of mouse IgM and IgA) or goat anti-rabbit IR800 (LI-COR Biosciences, number 926-32211, 1:15,000, reactive toward rabbit IgG heavy/light chains, rabbit IgM, and IgA light chains) secondary antibodies diluted in blocking buffer and imaged using LiCor Odyssey CLx Infrared Imaging System. The resulting images of immunoblots were imported into Empiria Studio (version 2.0) for analysis, where red (IR680) and green (IR800) channels were then separated and converted to grayscale for easier visualization. All raw and uncropped images of resulting immunoblots were included in Supplementary Figure S1.

### Statistical analysis

For quantification of signal intensity, fluorescently labeled images were converted to grayscale, with specific regions of interest highlighted to include epidermis and HF. Each image was segmented into 4−5 fields of view, with integrated density measured and divided by the area of each field of view, which was then averaged to provide a mean pixel intensity per image (see Supplementary Figure S2 for example quantification). Data were plotted as sample means, with error bars corresponding to SD from n = 3 biological replicates, and ordinary one-way ANOVA followed by Tukey's multiple comparison tests were used to assess statistical significance between normal skin, perilesional skin, and lesional HS samples (*$P < 0.05$, **$P < 0.01$, and ***$P < 0.001$) for each analyte (Cav1, Cav2, and Cavin-1).

### Data availability statement

No large datasets were generated or analyzed during this study. Minimal datasets necessary to interpret and/or replicate data in this paper are available upon request to the corresponding author.

### ORCIDs

Neil Seth: http://orcid.org/0009-0002-4257-1453
Beatriz Abdo Abujamra: http://orcid.org/0000-0001-8619-9273
Maria Boulina: http://orcid.org/0009-0001-7616-9668
Hadar Lev-Tov: http://orcid.org/0000-0001-6223-7001
Ivan Jozic: http://orcid.org/0000-0001-5114-9524

### AUTHOR CONTRIBUTIONS

Conceptualization: IJ, HL-T, MB; Methodology: NS, BAA; Formal Analysis: IJ, NS, BAA, MB; Resources: IJ, HL-T; Data Curation: IJ, BAA; Writing − Original Draft Preparation: NS, BAA, MB, HL-T, IJ; Writing − Review and Editing: NS, BAA, MB, HL-T, IJ

### REFERENCES

Amat-Samaranch V, Agut-Busquet E, Vilarrasa E, Puig L. New perspectives on the treatment of hidradenitis suppurativa. Ther Adv Chronic Dis 2021;12: 20406223211055920.

Cappilli S, Giovanardi G, Di Stefani A, Longo C, Perino F, Chiricozzi A, et al. Real-time confocal imaging for hidradenitis suppurativa: description of morphological aspects and focus on the role of follicular ostia. Dermatology 2021;237:705−11.

Castellanos A, Hernandez MG, Tomic-Canic M, Jozic I, Fernandez-Lima F. Multimodal, in situ imaging of ex vivo human skin reveals decrease of cholesterol sulfate in the neoepithelium during acute wound healing. Anal Chem 2020;92:1386−94.

Castelli E, Orlando E, Porcasi R, Tilotta G, Pistone G, Bongiorno MR, et al. Histopathological progression of hidradenitis suppurativa/acne inversa: a morphological study with a closer look on the early changes of the folliculosebaceous apocrine apparatus. Wien Med Wochenschr 2022;172: 126−34.

Chen W, Plewig G. Should hidradenitis suppurativa/acne inversa best be renamed as "dissecting terminal hair folliculitis"? Exp Dermatol 2017;26: 544−7.

Chidlow JH Jr, Sessa WC. Caveolae, caveolins, and cavins: complex control of cellular signalling and inflammation. Cardiovasc Res 2010;86:219−25.

Cohen AW, Hnasko R, Schubert W, Lisanti MP. Role of caveolae and caveolins in health and disease. Physiol Rev 2004;84:1341−79.

Egger AN, Rajabiestarabadi A, Williams NM, Resnik SR, Fox JD, Wong LL, et al. The importance of caveolins and caveolae to dermatology: lessons from the caves and beyond [published correction appears in Exp Dermatol 2020;29:446] Exp Dermatol 2020;29:136−48.

Emelianov VU, Bechara FG, Gläser R, Langan EA, Taungjaruwinai WM, Schröder JM, et al. Immunohistological pointers to a possible role for excessive cathelicidin (LL-37) expression by apocrine sweat glands in the pathogenesis of hidradenitis suppurativa/acne inversa. Br J Dermatol 2012;166:1023−34.

Frew JW, Navrazhina K, Byrd AS, Garg A, Ingram JR, Kirby JS, et al. Defining lesional, perilesional and unaffected skin in hidradenitis suppurativa: proposed recommendations for clinical trials and translational research studies. Br J Dermatol 2019;181:1339−41.

Garg A, Lavian J, Lin G, Strunk A, Alloo A. Incidence of hidradenitis suppurativa in the United States: a sex- and age-adjusted population analysis. J Am Acad Dermatol 2017;77:118−22.

Garrean S, Gao XP, Brovkovych V, Shimizu J, Zhao YY, Vogel SM, et al. Caveolin-1 regulates NF-kappaB activation and lung inflammatory response to sepsis induced by lipopolysaccharide. J Immunol 2006;177: 4853−60.

Ingram JR. The epidemiology of hidradenitis suppurativa. Br J Dermatol 2020;183:990−8.

Jemec GB, Kimball AB. Hidradenitis suppurativa: epidemiology and scope of the problem. J Am Acad Dermatol 2015;73:S4−7.

Jozic I, Abujamra BA, Elliott MH, Wikramanayake TC, Marjanovic J, Stone RC, et al. Glucocorticoid-mediated induction of caveolin-1 disrupts cytoskeletal organization, inhibits cell migration and re-epithelialization of non-healing wounds. Commun Biol 2021a;4:757.

Jozic I, Chéret J, Abujamra BA, Miteva M, Gherardini J, Paus R. A cell membrane-level approach to cicatricial alopecia management: is Caveolin-1 a viable therapeutic target in frontal fibrosing alopecia? Biomedicines 2021b;9:572.

Jozic I, Sawaya AP, Pastar I, Head CR, Wong LL, Glinos GD, et al. Pharmacological and genetic inhibition of Caveolin-1 promotes epithelialization and wound closure. Mol Ther 2019;27:1992−2004.

Kelly G, Hughes R, McGarry T, van den Born M, Adamzik K, Fitzgerald R, et al. Dysregulated cytokine expression in lesional and nonlesional skin in hidradenitis suppurativa. Br J Dermatol 2015;173:1431−9.

Kim YJ, Hirabayashi Y. Caveolin-1 prevents palmitate-induced NF-kappaB signaling by inhibiting GPRC5B-phosphorylation. Biochem Biophys Res Commun 2018;503:2673−7.

Moran B, Sweeney CM, Hughes R, Malara A, Kirthi S, Tobin AM, et al. Hidradenitis suppurativa is characterized by dysregulation of the Th17:Treg cell axis, which is corrected by anti-TNF therapy. J Invest Dermatol 2017;137:2389−95.

Napolitano M, Megna M, Timoshchuk EA, Patruno C, Balato N, Fabbrocini G, et al. Hidradenitis suppurativa: from pathogenesis to diagnosis and treatment. Clin Cosmet Investig Dermatol 2017;10:105−15.

Narla S, Lyons AB, Hamzavi IH. The most recent advances in understanding and managing hidradenitis suppurativa. F1000Res 2020;9:F1000.

Orvain C, Lin YL, Jean-Louis F, Hocini H, Hersant B, Bennasser Y, et al. Hair follicle stem cell replication stress drives IFI16/STING-dependent inflammation in hidradenitis suppurativa. J Clin Invest 2020;130:3777−90.

Parton RG, del Pozo MA. Caveolae as plasma membrane sensors, protectors and organizers. Nat Rev Mol Cell Biol 2013;14:98−112.

Riedemann NC, Habel M, Ziereisen J, Hermann M, Schneider C, Wehling C, et al. Controlling the anaphylatoxin C5a in diseases requires a specifically targeted inhibition. Clin Immunol 2017;180:25−32.

Sabat R, Jemec GBE, Matusiak Ł, Kimball AB, Prens E, Wolk K. Hidradenitis suppurativa. Nat Rev Dis Primers 2020;6:18.

Sawaya AP, Jozic I, Stone RC, Pastar I, Egger AN, Stojadinovic O, et al. Mevastatin promotes healing by targeting caveolin-1 to restore EGFR signaling. JCI Insight 2019;4:e129320.

Schneider-Burrus S, Tsaousi A, Barbus S, Huss-Marp J, Witte K, Wolk K, et al. Features associated with quality of life impairment in hidradenitis suppurativa patients. Front Med (Lausanne) 2021;8:676241.

Tsai TH, Tam K, Chen SF, Liou JY, Tsai YC, Lee YM, et al. Deletion of caveolin-1 attenuates LPS/GalN-induced acute liver injury in mice. J Cell Mol Med 2018;22:5573−82.

van der Zee HH, de Ruiter L, van den Broecke DG, Dik WA, Laman JD, Prens EP. Elevated levels of tumour necrosis factor (TNF)-α, interleukin (IL)-1β and IL-10 in hidradenitis suppurativa skin: a rationale for targeting TNF-α and IL-1β. Br J Dermatol 2011;164:1292−8.

von Laffert M, Helmbold P, Wohlrab J, Fiedler E, Stadie V, Marsch WC. Hidradenitis suppurativa (acne inversa): early inflammatory events at terminal follicles and at interfollicular epidermis. Exp Dermatol 2010;19:533−7.

Wang XM, Kim HP, Nakahira K, Ryter SW, Choi AM. The heme oxygenase-1/carbon monoxide pathway suppresses TLR4 signaling by regulating the interaction of TLR4 with caveolin-1. J Immunol 2009;182:3809−18.

Wolk K, Join-Lambert O, Sabat R. Aetiology and pathogenesis of hidradenitis suppurativa. Br J Dermatol 2020;183:999−1010.

Yu CC, Cook MG. Hidradenitis suppurativa: a disease of follicular epithelium, rather than apocrine glands. Br J Dermatol 1990;122:763−9.

Zouboulis CC, Nogueira da Costa A, Fimmel S, Zouboulis KC. Apocrine glands are bystanders in hidradenitis suppurativa and their involvement is gender specific. J Eur Acad Dermatol Venereol 2020;34:1555−63.
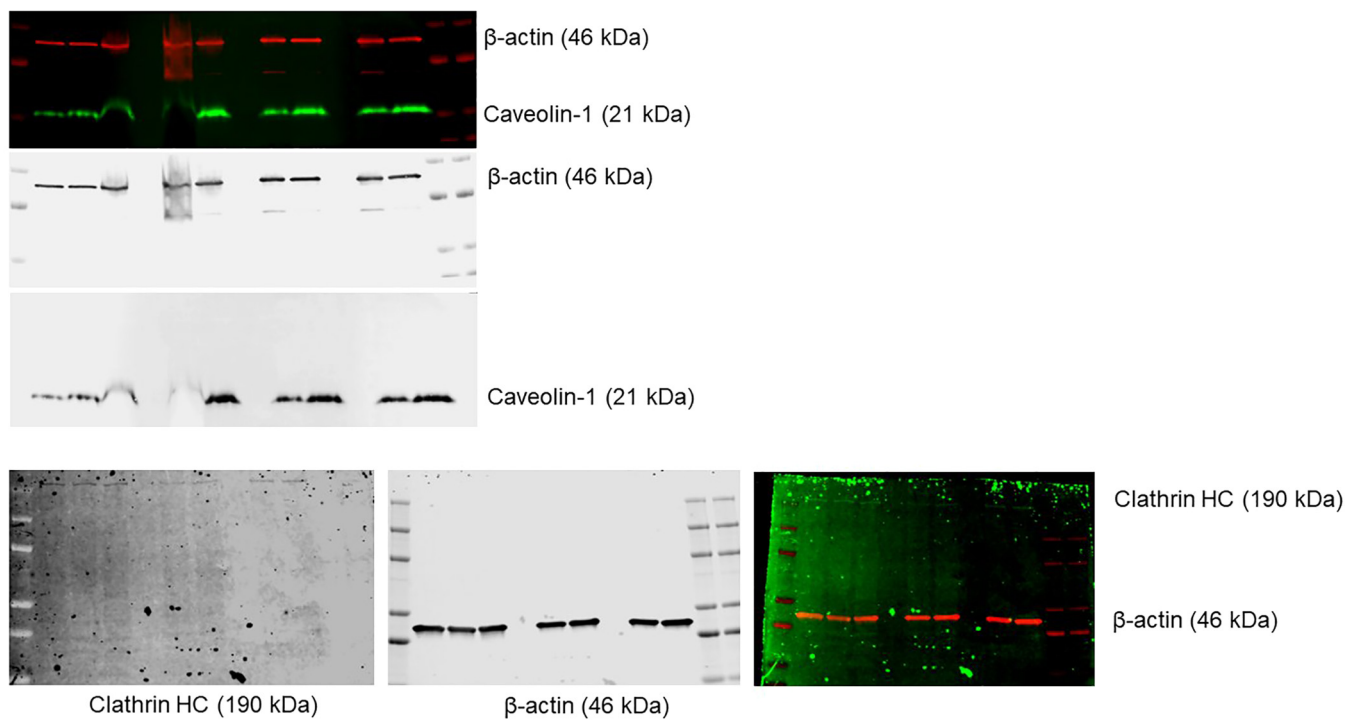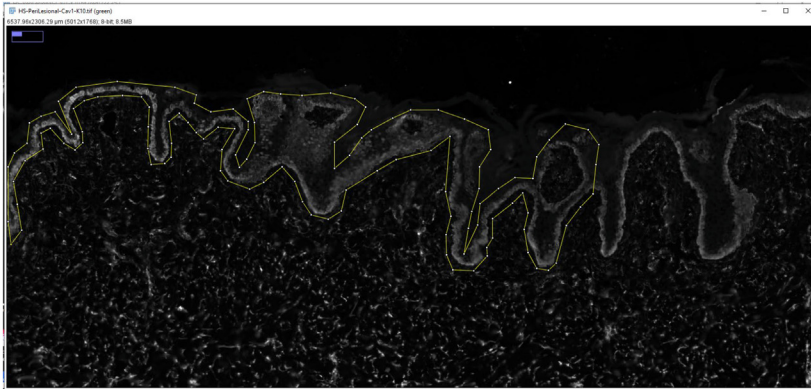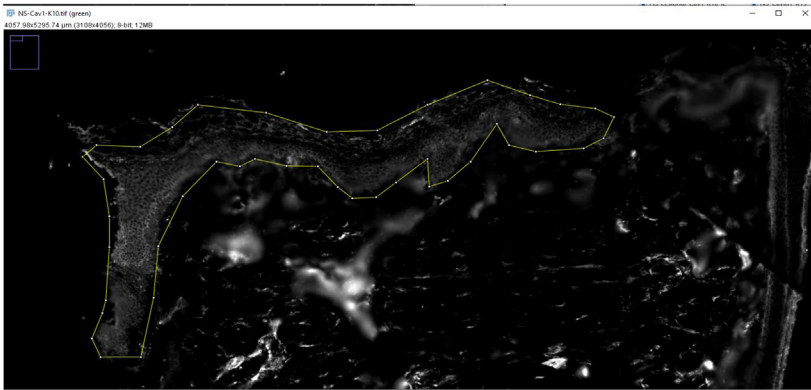
**Supplemental Figure S1. Uncropped images of immunoblots from Figure 5.** Images of immunoblots were captured using LiCor Odyssey CLx Infrared Imaging System, with red and green channels separated and converted to grayscale images for easier visualization. HC, heavy chain.
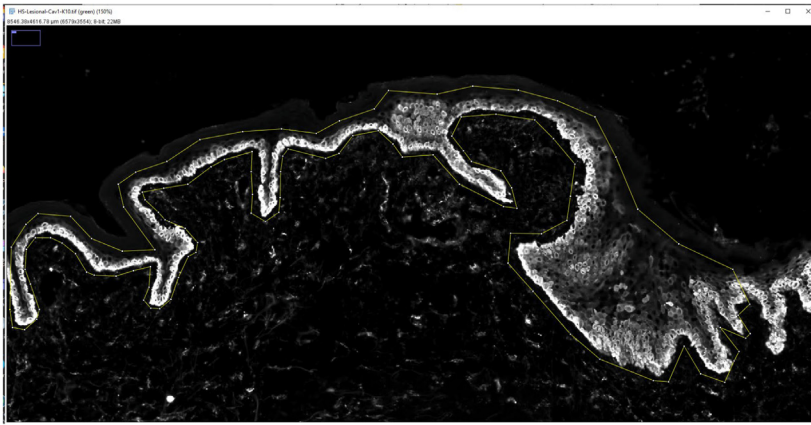
| Lesional | Int density | Area | Pixel density over area |
|---|---|---|---|
| | 7893646.361 | 94935.46 | 83.15 |
| | 16426597.63 | 216160.5 | 75.99 |
| | 10952524.78 | 145047.5 | 75.51 |
| | 15853361.78 | 283493.5 | 55.92 |
| | 12696549.22 | 267593.9 | 47.45 |
| | | | |
| | | Average | 67.60 |



| Peri lesional | Int density | Area | Pixel density over area |
|---|---|---|---|
| | 9957717.146 | 333629.7 | 29.85 |
| | 8222727.52 | 239703.7 | 34.30 |
| | 14474464.45 | 316097.9 | 45.79 |
| | 7144807.928 | 174710.3 | 40.90 |
| | | | |
| | | Average | 37.71 |



| Normal skin | Int density | Area | Pixel density over area |
|---|---|---|---|
| | 5937031.045 | 301600.1 | 19.69 |
| | 4742434.262 | 210326.9 | 22.55 |
| | 6403463.577 | 249646.3 | 25.65 |
| | 4485133.719 | 224868.6 | 19.95 |
| | | | |
| | | Average | 21.96 |

**Supplemental Figure S2. Sample pixel intensity quantification for Cav1 staining of normal skin, lesional skin, and perilesional HS samples.** Fluorescently labeled images were converted to grayscale, with specific regions of interest highlighted to include the epidermis and hair follicle. Each image was segmented into 4−5 fields of view with integrated density measured and divided by the area of each field of view, which was then averaged to provide a mean pixel intensity per image. Cav1, caveolin-1; HS, hidradenitis suppurativa.